

# Random Number Generator and Secure Communication Applications Based on Infinitely Many Coexisting Chaotic Attractors

Abdullah Noor , Zehra Gülru Çam Taşkıran 

Department of Engineering, Yıldız Technical University, Institute of Science, İstanbul, Turkey

**Cite this article as:** A. Noor, Z. G. Çam Taşkıran, "Random Number Generator and SecCure Communication Applications Based on Infinitely Many Coexisting Chaotic Attractors", *Electrica*, vol. 21, no. 2, pp. 180-188, May, 2021.

## ABSTRACT

This paper aims to investigate a 3D chaotic system for applications on the secure communication system and random number generation. There exists a sinusoidal nonlinearity in the system making it uncommon of its type. Infinitely many chaotic attractors indicate multi-stability of the system, which is desired; for instance, the same system can be implemented for a multiple channel secure communication and switching between the channels can be achieved just by changing initial conditions. A brief mathematical analysis of the system is performed, and the circuit of the system is designed using active circuit elements. A synchronized system for secure communication is mathematically analyzed on MATLAB and simulated on PSPICE OrCAD. Synchronization of the system with the proposed circuit structure shows that this dynamic system can be used for chaotic communication. In addition, as an application of cryptography, a NIST\* statistical test is performed on 10 bitstreams generated by the system. The bitstream produced has successfully passed all tests giving results in the length of the generated bit.

**Keywords:** Chaotic Circuit, chaotic masking, secure communication, random number generator

## Corresponding Author:

Zehra Gülru Çam Taşkıran

## E-mail:

zgcam@yildiz.edu.tr

**Received:** February 16, 2021

**Accepted:** April 20, 2021

**DOI:** 10.5152/electrica.2021.21017



Content of this journal is licensed under a Creative Commons Attribution-NonCommercial 4.0 International License.

## Introduction

Lorenz's [1] publication entitled "Does the flap of a butterfly's wings in Brazil set off a Tornado in Texas" was inspired by the basic characteristic of the chaotic systems. Lorenz observed extreme sensitivity of the chaotic systems to their initial conditions while performing weather simulations.

The fact that most of the real-world problems are nonlinear, with the discovery and the mathematical description of a simple chaotic system by Lorenz [2] has given the research on dissipative dynamical systems a new direction. Chaos theory, owing to its complex dynamics, has found applications in almost all the fields of life, including biology and medicine [3], management in industry [4], learning in classroom [5, 6], psychology [7], supply chain managements [8], and transportation [9, 10]. Chaos was thought undesirable and uncontrollable for some time but as the research moved from analysis to control of the chaotic systems [11-15], many novel chaotic systems are discovered and analyzed [16-21].

Cryptography is the combination of a Random Number Generator (RNG) and an encryption algorithm. Chaotic signals are applied widely in cryptography where random numbers are acting as fundamental units [23-29]. Demir and Ergün [30] performed analysis of deterministic chaos, generated by a phase-locked loop device and showed that unbounded chaos and Gaussian white noise are comparable as an entropy source; the same authors demonstrated some security vulnerabilities of the cryptography (RNG and XOR encryption algorithm) based on a 4D chaotic hyperjerk system [31]. Tutueva et al. [32] proposed Adaptive Zaslavsk web maps for generation of pseudorandom numbers (PRN) to improve chaos-based cryptography. Another efficient digital image encryption algorithm utilizing PRN generator, based on chaotic fractal sequence was proposed by Ayubi et al. [33]. Sprött and Thio [34] generated Gaussian Random Numbers with a simple chaotic circuit.

Chaotic signals have broadband and noise-like spectrum; hence, chaotic systems synchronize only with their selves [35] and are very practical for communication systems. After the proof of experimental feasibility of the chaotic systems for communication [15], many chaotic systems are synchronized using different synchronization algorithms. Sundarapandian and Pehlivan [17], achieved adaptive synchronization of a novel chaotic system with its realization in PSpice. Sundarapandian et al. [21] applied a new complex 3D chaotic system on an autonomous wireless mobile robot and realized its circuit on MultiSIM10. Herman Sedef and others synchronized and simulated the Lorenz system with two different methods [36-38].

In this study, a recently reported chaotic system having infinitely many coexisting attractors is a matter of concern for RNG and secure communication system [22]. Synchronization in this study is achieved by the addition of a difference term, a method introduced by Sambas et al. [38]. Random 10 bitstream is generated by performing XOR operation on two different signals of the system, and the randomness of the generated sequence is proved with NIST statistical test [39].

**System**

In this study, an extremely simple chaotic system with infinitely many coexisting chaotic attractors, which is defined as in (1) consisting of five terms with two nonlinearities, has been analyzed and applied for RNG and secure chaotic communication [22].

$$\dot{x}_1 = a(x_2 - x_1) \tag{1a}$$

$$\dot{x}_2 = bx_1 \sin(x_3) \tag{1b}$$

$$\dot{x}_3 = c - x_1x_2 \tag{1c}$$

$x_1, x_2,$  and  $x_3$  are state variables and  $a, b,$  and  $c$  are positive constants. Two nonlinearities of the system are  $x_1$  and  $x_1x_2,$  respectively.

**Mathematical Analysis**

Jacobian matrix, Lyapunov exponents, bifurcation diagram, phase portrait, and time series analysis are some of the important methods to verify and control the chaoticity of any system. These methods are briefly studied. Sinusoidal nonlinearity of the system (1) indicates an infinite number of unstable equilibria.

by  $\dot{x}_1 = \dot{x}_2 = \dot{x}_3 = 0,$  resulting equilibrium of the system (1)

$$\begin{aligned} (1a) &\Rightarrow x_2 = x_1 \\ (1b) &\Rightarrow x_3 = \sin^{-1}(0) = k\pi \quad \text{where } k = 0, \pm 1, \pm 2, \pm 3, \dots \\ (1c) &\Rightarrow x_1x_2 = c \Rightarrow x_2 = x_1 = \pm\sqrt{c} \end{aligned}$$

$$O = \{(\dot{x}_1, \dot{x}_2, \dot{x}_3) \mid x_2 = x_1 = \pm\sqrt{c}, x_3 = k\pi\}$$

System (1) is multistable because of the coexistence of attractors and its final state is decided by initial conditions [40]. Jacobian matrix gives vital information for the analysis of a chaotic system.

$$J = \begin{bmatrix} \frac{\partial \dot{x}_1}{\partial x_1} & \frac{\partial \dot{x}_2}{\partial x_1} & \frac{\partial \dot{x}_3}{\partial x_1} \\ \frac{\partial \dot{x}_1}{\partial x_2} & \frac{\partial \dot{x}_2}{\partial x_2} & \frac{\partial \dot{x}_3}{\partial x_2} \\ \frac{\partial \dot{x}_1}{\partial x_3} & \frac{\partial \dot{x}_2}{\partial x_3} & \frac{\partial \dot{x}_3}{\partial x_3} \end{bmatrix} = \begin{bmatrix} -a & a & 0 \\ b \sin(x_3) & 0 & bx_1 \cos x_3 \\ -x_2 & -x_1 & 0 \end{bmatrix}$$

resulting gradient of system  $\nabla V = \frac{\partial \dot{x}_1}{\partial x_1} + \frac{\partial \dot{x}_2}{\partial x_2} + \frac{\partial \dot{x}_3}{\partial x_3} = -a.$

Gradient  $\nabla V < 0$  is a necessary condition for any system to be chaotic. Therefore, for any positive value of "a", system (1) will show chaotic behavior given suitable initial conditions and its phase space will become wider continuously [41].

Bifurcation diagram shows the ranges of a dynamical system for chaoticity, periodicity, and quasi periodicity, under the condition that one of the parameters (bifurcation parameter) is not fixed. By utilizing this information, we can generate the desired behavior of our system. The bifurcation diagram of system (1) with respect to the parameter  $c \in (0, 1)$  taking  $a = 1$  and  $b = 12$  is shown in Figure 1. The system (1) is periodic for a wide range of  $c > 0.7,$  chaotic for  $0 < c < 0.55,$  and quasi periodic for  $0.55 < c < 0.7$  approximately.

Lyapunov exponents or Lyapunov characteristic exponents of a dynamical system are the rates of convergence or divergence of infinitesimally nearby orbits. Lyapunov exponent for constant parameters of  $a = 1, b = 12,$  and  $c = 0.30$  (chaotic range) is resulting (+,0,-) exponents (Figure 2a) and for  $c=1$  (periodic range) is resulting (0,-,-) exponents (Figure 2b), given initial conditions of [1, 0, 1]. In the prior case, the largest exponent is positive, verifying the chaoticity and the sensitivity of system (1) to initial conditions [42, 44]. In the latter case, the largest Lyapunov exponent is zero so the system will become independent of the initial conditions over time [43].

3D projections of phase space are observed for the initial conditions of  $\{x_2 = x_1 = 1, x_3 = s\pi \mid s = 2, 4, 6, 8, 10, 12\}$  and with the constant parameters  $a = 1, b = 12.$  Closed curves for  $c = 1$  in Figure 3a represent periodic systems, whereas complex shapes for  $c = 0.3$  in Figure 3b are of chaotic systems.

Finally, the chaoticity of the system is verified by analysis of the time series. Analyzing a system in the time domain is an easy way to determine whether a system is periodic or not. It can be verified from Figure 4a that for  $c = 1,$  system is in the periodic region and for  $c = 0.3,$  system is in chaotic region Figure 4b.

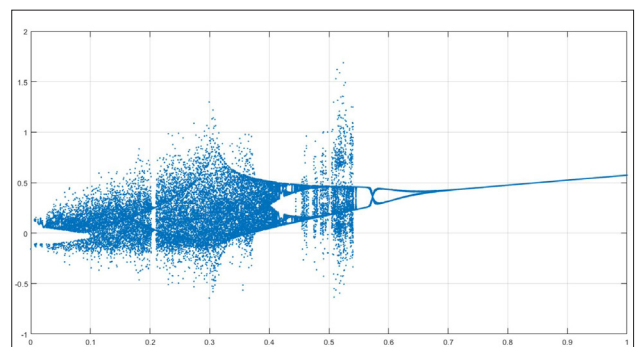


**Figure 1.** Bifurcation diagram for  $c \in (0, 1), a = 1$  and  $b = 12$

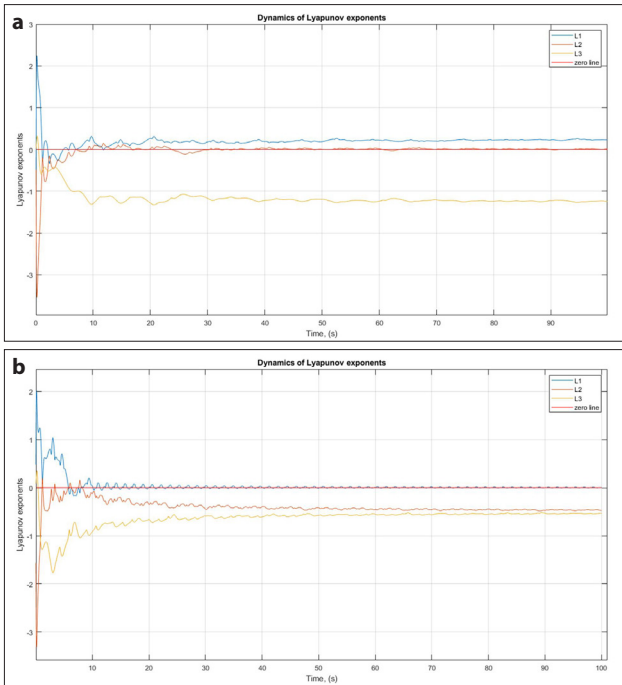


**Figure 2. a, b.** Chaotic state Lyapunov exponents (a). Periodic state Lyapunov exponents (b)

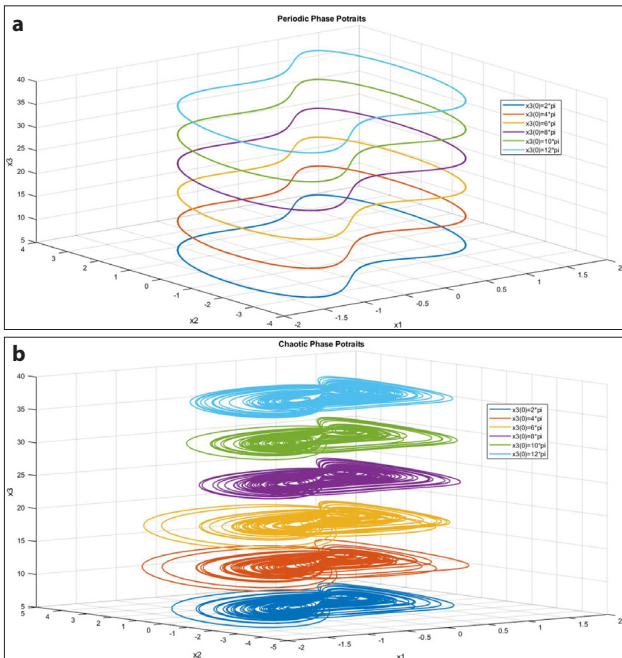


**Figure 3. a, b.** Periodic state phase portraits (a). Chaotic state phase portraits (b)

**Circuit Design Using Active Elements**

Parallel synthesis method using op amp circuits have been used for circuit realization in past studies. However, a higher number of active and passive elements have many disadvantages including higher power consumption, system complexity, and difficulty to

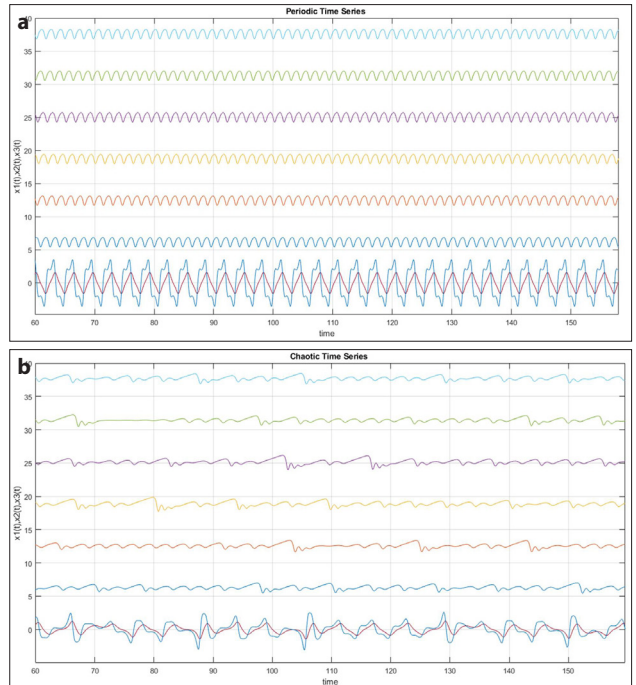


**Figure 4. a, b.** Periodic time-series for  $\{x_2=x_1=1, x_3= s\pi |s=2, 4, 6, 8, 10, 12\}$  (a). Chaotic time-series for  $\{x_2=x_1=1, x_3= s\pi |s=2, 4, 6, 8, 10, 12\}$  (b)

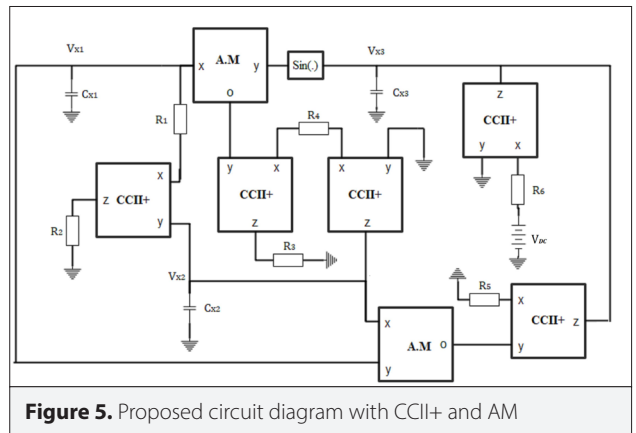


**Figure 5.** Proposed circuit diagram with CCII+ and AM

control. Therefore, to avoid these problems, circuit of the system (1) is designed using alternative active elements i.e., second generation current conveyors (CCII+) and analog multipliers (AM). The circuit diagram of the system is shown in Figure 5. Using the proposed circuit, the number of active elements was reduced from 9 to 7 and the number of passive elements was reduced from 12 to 9.

By applying basic circuit analysis on the circuit diagram, system equations are derived as (2).

**Kirchhoff's Current Law at node Vx1**

$$c_{x1} \frac{dv_{x1}}{dt} = \frac{v_{x2} - v_{x1}}{R_1} \Rightarrow \frac{dx_1}{dt} = \frac{(v_{x2} - v_{x1})}{R_1 * c_{x1}} \tag{2.1}$$

**Kirchhoff's Current Law at node Vx2**

$$c_{x_2} \frac{dv_{x_2}}{dt} = \frac{kv_{x_1} \sin v_{x_3}}{R_4} \Rightarrow \frac{dv_{x_2}}{dt} = \frac{kv_{x_1} \sin v_{x_3}}{R_4 * c_{x_2}} \quad (2.2)$$

**Kirchhoff's Current Law at node Vx3**

$$c_{x_3} \frac{dv_{x_3}}{dt} = \frac{V}{R_6} - \frac{kv_{x_1} * v_{x_2}}{R_5} \Rightarrow \frac{dv_{x_3}}{dt} = \frac{V}{c_{x_3} * R_6} - \frac{kv_{x_1} * v_{x_2}}{c_{x_3} * R_5} \quad (2.3)$$

By assuming  $\frac{dv_{x_1}}{dt} = \dot{x}_1, \frac{dv_{x_2}}{dt} = \dot{x}_2, \frac{dv_{x_3}}{dt} = \dot{x}_3, v_{x_1} = x_1, v_{x_2} = x_2, v_{x_3} = x_3, a = \frac{1}{R_1 c_{x_1}}$ ,  $b = \frac{k}{c_{x_2} * R_4}$   $c = \frac{V}{R_6 c_{x_3}}$  and  $\frac{k}{c_{x_3} * R_5} = 1$ , it can be proved that system (2) is equivalent to system (1).

Values of the circuit elements, calculated by assuming  $a = 1, b = 12, c = 0.3$ , and  $k = 0.1$  are given in Table 1. DC voltage source  $VDC = 30\text{ mV}$  for constant parameter  $c$ .

**Table 1.** Calculated values of circuit elements

Element	$R_1$	$R_4$	$R_5$	$R_6$
Value	$5\text{ k}\Omega$	$5\text{ k}\Omega$	$5\text{ k}\Omega$	$5\text{ k}\Omega$
Element	$C_{x_1}$	$C_{x_2}$	$C_{x_3}$	$k$
Value	$200\ \mu\text{F}$	$1.667\ \mu\text{F}$	$20\ \mu\text{F}$	$0.1\text{ V}^{-1}$

To operate the system in realizable range amplitude, scaling coefficient  $K_a$  and frequency scaling coefficient  $K_f$  are taken as 0.01 and 1000, respectively, resulting in denormalized elements values of  $R = 50, C_{x_1} = 20\ \mu\text{F}, C_{x_2} = 0.1667\ \mu\text{F}$ , and  $C_{x_3} = 2\ \mu\text{F}$ . Pspice macro-models of commercially available integrated circuits are used for PSpice simulation. AD633 [44] integrated circuit is used for AM, whereas AD844 [45] is used for CCI+ by keeping w port as an open circuit. Comparison of 2D phase portraits and time series generated from the mathematical analyzes in MATLAB and simulation in PSpice are given in Figure 6 and Figure 7, respectively.

**Chaotic Synchronization**

As a practical application, the communication system is synchronized by adding a difference term; this method presented in [38]. Below are the system equations of the transmitter (3), the receiver (4), and message signal (5) derived from the circuit diagram of the communication system given in Figure 8. The advantage of this method over the other widely used methods [37] is that the synchronization signal does not need to be sent continuously. As the difference term in (4.3) will be zero after the systems are synchronized, transfer of the synchronization signal  $x_3$  can be stopped, thus continuing communication with only one channel.

$$\dot{x}_1 = \frac{(x_2 - x_1)}{R_1 * c_{x_1}} \quad (3.1)$$

$$\dot{x}_2 = \frac{kx_1 \sin x_3}{R_4 * c_{x_2}} \quad (3.2)$$

$$\dot{x}_3 = \frac{V}{c_{x_3} * R_6} - \frac{kx_1 x_2}{c_{x_3} * R_5} \quad (3.3)$$

$$\dot{x}_4 = \frac{(x_5 - x_4)}{R_1 * c_{x_1}} \quad (4.1)$$

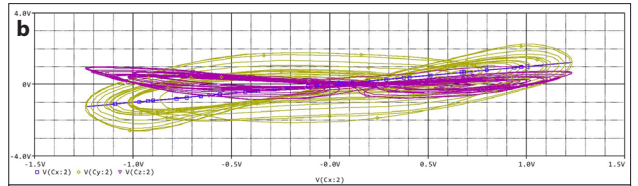
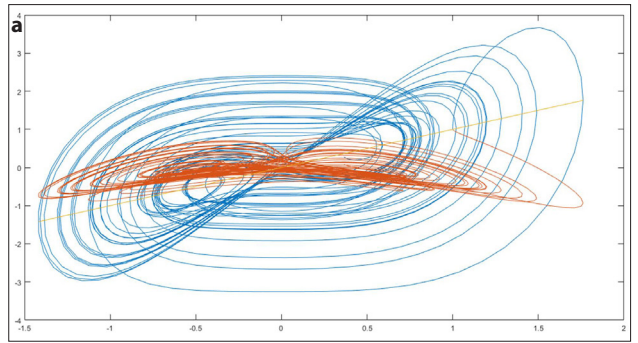


**Figure 6. a, b.** Phase Portrait obtained mathematically in MATLAB (a). Phase Portraits obtained with simulation in PSpice (b)

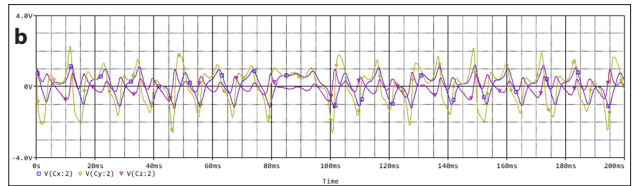
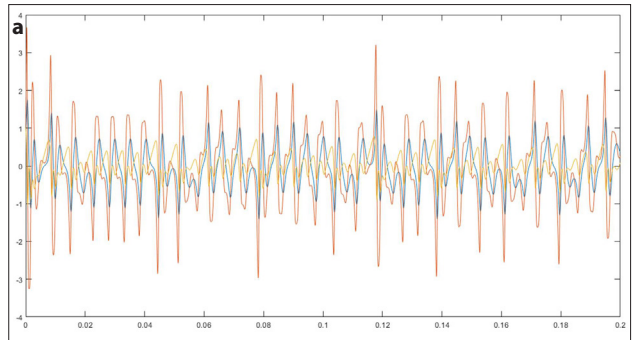


**Figure 7. a, b.** Time-series obtained in MATLAB (a). Time-series obtained with simulation in PSpice (b)

$$\dot{x}_5 = \frac{kx_4 \sin x_6}{R_4 * c_{x_2}} \quad (4.2)$$

$$\dot{x}_6 = \frac{V}{c_{x_3} * R_6} - \frac{kx_4 x_5}{c_{x_3} * R_5} + \frac{(x_3 - x_6)}{R_7 * c_{x_3}} \quad (4.3)$$

$$\dot{m} = -A * \omega * \sin(\omega t) \quad (5)$$

In this system, after the receiver and transmitter are synchronized by using  $x_3$  signal, namely  $V_x$ , the information signal to be transmitted is added to  $x_1, V_x$  on the receiver side, and sent to the receiver through the communication channel. As the  $V_x$  signal is produced exactly on the receiver side (as  $x_4$ ), the original information message ( $m(t)$ ) is obtained by subtracting the  $V_x$  on the receiver side from the received signal. The block diagram of the method is given in Figure 9.

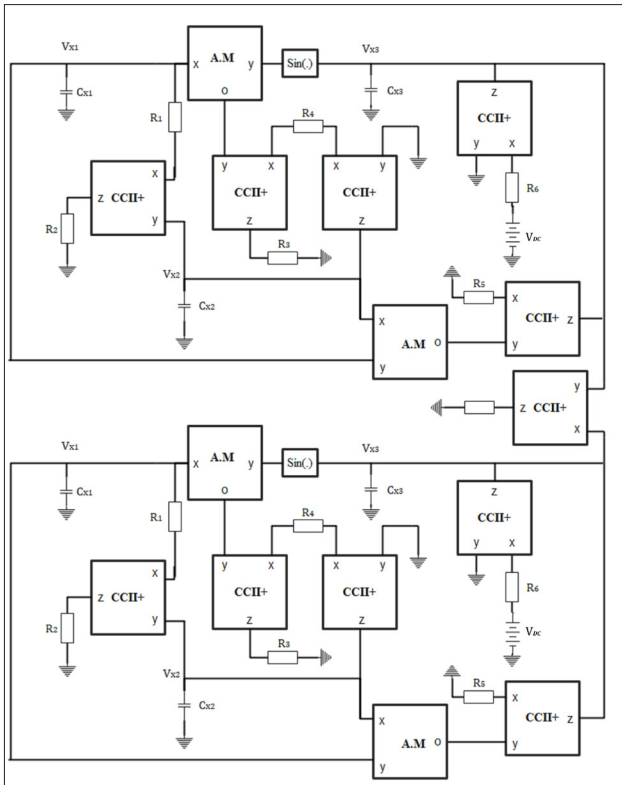


**Figure 8.** Synchronization of transmitter and receiver circuits by using difference adding method

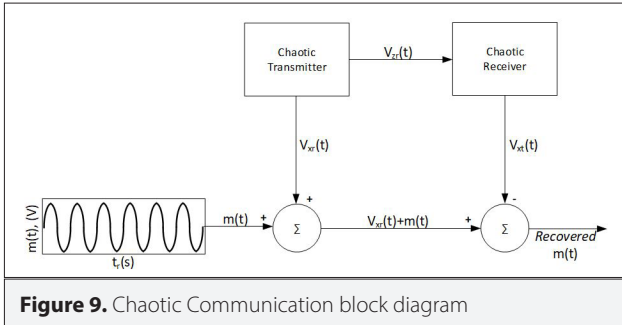


**Figure 9.** Chaotic Communication block diagram

By setting  $\omega=2*\pi*40$  and value of difference term coefficient as -300, the system gets synchronized after approximately 120 ms in MATLAB and it takes approximately 160 ms in PSpice. Comparison of received versus transmitted  $V_z$  ( $x_3$  and  $x_6$ ) drawn by MATLAB and PSpice simulation is provided in Figure 10a and Figure 10b, respectively. Initial conditions for transmitter circuit are (1,1,1) and for receiver circuit are (1,1,0). Comparison of transmitted and received messages plotted in MATLAB is provided in Figure 11a and 11b.

Furthermore, the system is synchronized using another method, signal transfer [35].  $x_2$  is selected as the signal to be transferred, and  $V_x$  ( $x_1$  and  $x_4$ ) signals initiated from different initial conditions are observed. Initial conditions for transmitter circuit are (1,1,1) and for receiver circuit are (0,1,1.2). Equations

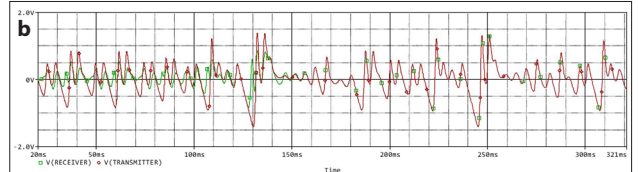
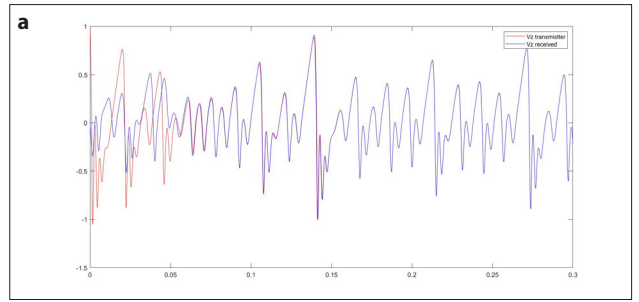


**Figure 10. a, b.** Transmitter and Receiver  $V_z$  in MATLAB for difference adding method (a). Transmitter and Receiver  $V_z$  in PSpice OrCAD for difference adding method (b)

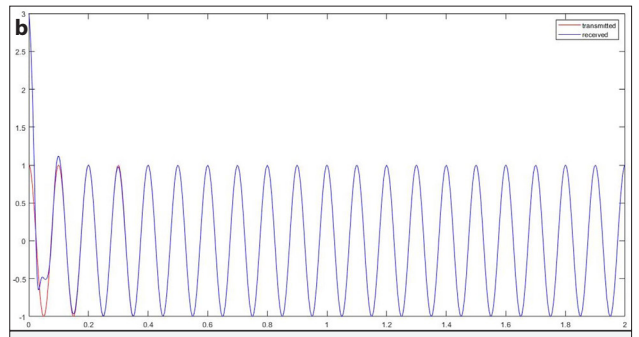
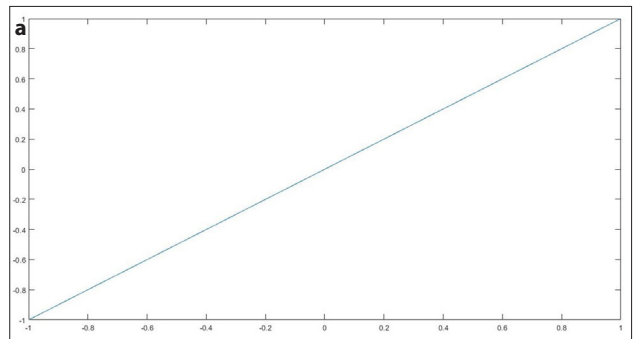


**Figure 11. a, b.** Transmitted vs. received message (a). Transmitted and received signal in time domain (b)

used for receiver and transmitter circuits are given in (6) and (7), respectively.

$$\dot{x}_1 = \frac{(x_2 - x_1)}{R_1 * c_{x1}} \quad (6.1)$$

$$\dot{x}_2 = \frac{kx_1 \sin x_3}{R_4 * c_{x2}} \quad (6.2)$$

$$\dot{x}_3 = \frac{V}{c_{x3} * R_6} - \frac{kx_1 x_2}{c_{x3} * R_5} \quad (6.3)$$

$$\dot{x}_4 = \frac{(x_2 - x_4)}{R_1 * c_{x1}} \quad (7.1)$$

$$\dot{x}_5 = \frac{kx_4 \sin x_6}{R_4 * c_{x2}} \quad (7.2)$$

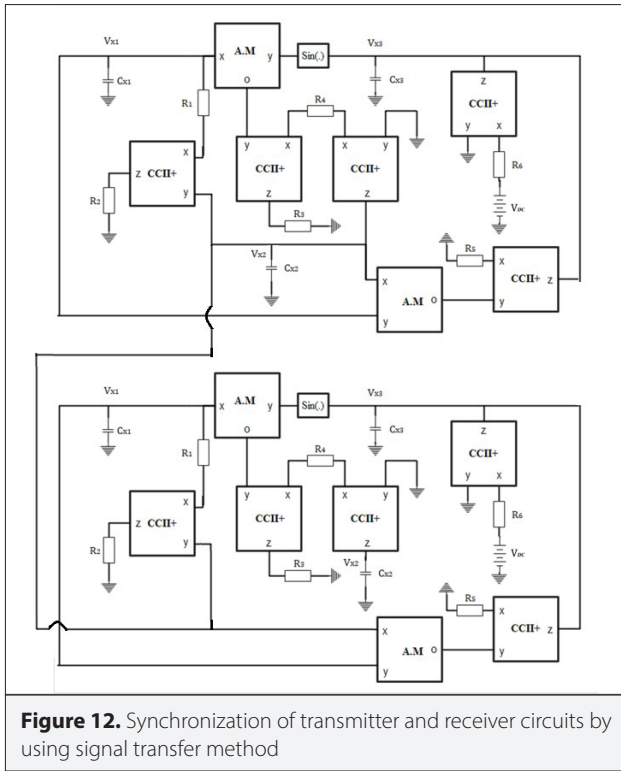


**Figure 12.** Synchronization of transmitter and receiver circuits by using signal transfer method

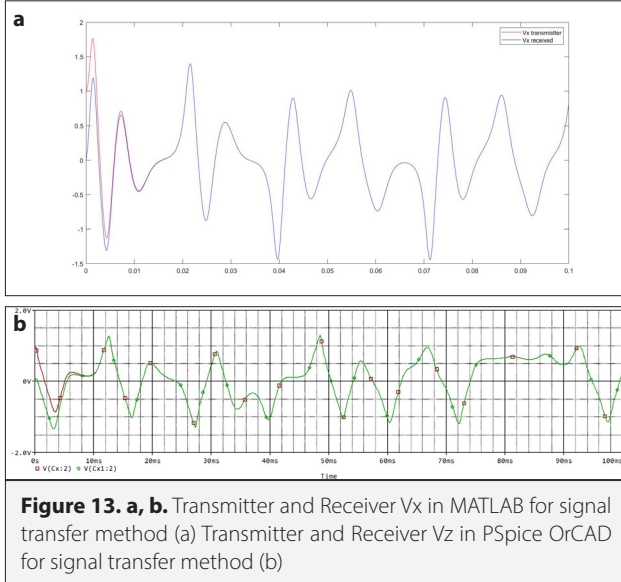


**Figure 13. a, b.** Transmitter and Receiver  $V_x$  in MATLAB for signal transfer method (a) Transmitter and Receiver  $V_z$  in PSpice OrCAD for signal transfer method (b)

$$\dot{x}_6 = \frac{V}{c_{x3} * R_6} - \frac{kx_4 x_2}{c_{x3} * R_5} \quad (7.3)$$

The block diagram of the method is given in Figure 12. The mathematical analysis of  $V_x(x_1 \text{ and } x_4)$  signals drawn by MATLAB is given in Figure 13a. The simulation results obtained are given in Figure 13b. The system gets synchronized after approximately 15 ms in MATLAB and it takes approximately 10 ms in PSpice. With this method, the system is synchronized relatively faster. Besides, there is no need to use an extra active and passive element.

**Table 2.** NIST test results

Statistical test	p value	p value (KS)	Proportion
Frequency	0.066882	0.031899	1.0000
Block frequency M = 128	0.739918	0.364893	1.0000
Cumulative sums (forward)	0.534146	0.495070	1.0000
Cumulative sums (reverse)	0.213309	0.261194	0.9000
Runs	0.350485	0.107286	1.0000
Longest run	0.350485	0.493332	1.0000
Rank	0.213309	0.393105	1.0000
FFT	0.350485	0.928316	1.0000
Nonoverlapping template (min) M = 9	0.008879	0.015736	0.9000
Nonoverlapping template (max) M = 9	0.991468	0.853972	1.0000
Overlapping template M = 9	0.350485	0.682616	0.9000
Approximate entropy M = 10	0.739918	0.799079	0.9000
Serial(1) M = 16	0.350485	0.810288	1.0000
Serial(2) M = 16	0.350485	0.438950	1.0000
Linear complexity M = 500	0.911413	0.769873	1.0000

### RNG

For the RNG, samples were obtained from the  $x_1$  and  $x_3$  time series produced by the chaotic generator, with the sampling frequency of 0.78 Hz. If the sample taken is a positive value, logic 1 information is recorded otherwise logic 0 information is recorded. A bit sequence is obtained by applying XOR operation to these logical values. The length of the resulting bitstream is 309 360. For NIST tests, 10 bitstreams were obtained. Used NIST parameters are taken for Block Frequency Test - block length as 128, Overlapping Template Test - block length as 9, Approximate Entropy Test - block length as 10, Serial Test - block length(m) as 16, and Linear Complexity Test - block length as 500. These arrays were NIST [39] tested for randomness control. The bitstreams have passed all the tests, available for the bitstreams of provided length. The NIST test results are given in Table 2. In this way, the resulting random bitstream can be used in image encryption methods that require random bits [46]. The RNGs obtained by solving the equations algorithmically

are called pseudo random number generators (PRNG), whereas the generators that are based on hardware and can be affected by environmental factors are called true RNGs (TRNGs). It has been shown that a TRNG can be obtained by implementing the proposed circuit in hardware with proposed integrated circuits and passive circuit elements.

## Conclusion

According to the schematic diagram of the circuit in the article in which the equation set is referenced [22], a structure containing fewer active elements is proposed in this study. However, the sine block used in the diagram is not a physically available active element. Therefore, in the reference study, physical realization has been made with a microcontroller by using digital realization instead of analog. However, there are studies in the literature that include current-mode elements and chaotic oscillator implementation and mention the advantages of current-mode operation [47]. In a similar study based on CCII+, an alternative to the Chua oscillator structure [48], which is widely used in the literature, is proposed. Although Chua diode structure can be realized with five active elements based on op amps [49], the nonlinear term can be produced with 2 CCII+ elements in the study. This study aims to emphasize the advantages of CCII+ based structures compared to the classical op amp-based structure. This advantage is to save space with the ability to create structures with fewer active and passive elements.

In this study, all mathematical analyses and simulation results are in good agreement. Successful chaotic synchronization has been achieved in MATLAB and PSpice simulations using two different synchronization methods. Bitstreams generated from XOR of two signals passed all the NIST tests. Thus, the system is feasible to use in chaotic encryption algorithms and secure communication.

**Peer-review:** Externally peer-reviewed.

**Author Contributions:** Concept – Z.G.Ç.T.; Design – Z.G.Ç.T.; Supervision – Z.G.Ç.T.; Resources – Z.G.Ç.T., A.N.; Materials – Z.G.Ç.T., A.N.; Data Collection and/or Processing – A.N.; Analysis and/or Interpretation – A.N.; Literature Search – A.N.; Writing Manuscript – Z.G.Ç.T., A.N.; Critical Review – Z.G.Ç.T., A.N.; Other – Z.G.Ç.T., A.N..

**Conflict of Interest:** The authors have no conflicts of interest to declare.

**Financial Disclosure:** The authors declared that this study has received no financial support.

## References

1. E. N. Lorenz, "Hvad er matematik?", American Association for the Advancement of Science, 1972.
2. E. N. Lorenz, "Deterministic Nonperiodic Flow," *J Atmospheric Sci*, vol. 20, pp. 130-141, 1963. [\[Crossref\]](#)
3. J. E. Skinner, M. Molnar, T. Vybiral, M. Mitra, "Application of Chaos Theory to Biology and Medicine", *Integr Physiol Behav Sci*, vol. 27, no. 1, pp. 39-53, 1992. [\[Crossref\]](#)
4. D. Levy, "Chaos Theory and Strategy: Theory Application, and managerial Implication," *Strategic Manag J*, vol. 15, pp. 167-178, 1994. [\[Crossref\]](#)
5. J. Trygstad, "Chaos in the Classroom: An Application of Chaos Theory," Paper presented at the Annual Meeting of the American Educational Research Association, Chicago, 1997.
6. V. Akmansoy, S. Kartal, "Chaos Theory and its Application to Education: Mehmet Akif Ersoy University Case," *Educational Sciences: Theory & Practice*, vol. 14, no. 2, pp. 510-518, 2014. [\[Crossref\]](#)
7. S. Ayers, "The Application of Chaos Theory to Psychology", *Theory & Psychology*, vol. 7, no. 3, pp. 373-398, 1997. [\[Crossref\]](#)
8. D. Stapleton, J. B. Hanna, R. R. Jonathan, "Enhancing supply chain solutions with the application of chaos theory", *Supply Chain Management: An International J*, vol. 11, no. 2, pp. 108-114, 2006. [\[Crossref\]](#)
9. A. Adewumi, J. Kagamba, A. Alochukwu, "Application of Chaos Theory in the Prediction of Motorised Traffic Flows on Urban Networks", *Mathematical Problems in Engineerin*, vol. 2016, p. 15, 2016. [\[Crossref\]](#)
10. C. Frazier, K. M. Kockelman, "Chaos Theory and Transportation Systems", *J Transportation Res Board*, vol. 1897, p. 9-17, 2004. [\[Crossref\]](#)
11. L. M. Pecora, T. L. Carroll, "Synchronization in Chaotic Systems," *Physical Rev Lett*, vol. 64, no. 8, 1990. [\[Crossref\]](#)
12. E. Ott, C. Grebogi, J. A. Yorke, "Controlling Chaos", *Physical Rev Lett*, vol. 64, no. 11, pp. 1196-1199, 1990. [\[Crossref\]](#)
13. K. Pyragas, "Continuous control of chaos by self-controlling feedback", *Physics Letters A*, vol. 170, no. 6, pp. 421-428, 1992. [\[Crossref\]](#)
14. S. Troy, C. Grebogi, E. Ott, J. A. Yorke, "Using Small Perturbations to Control Chaos", *Nature*, vol. 363, pp. 411-417, 1993. [\[Crossref\]](#)
15. S. Hayes, C. Greboi, E. Ott, A. Mark, "Experimental Control of Chaos for Communication", *Physical Rev Lett*, vol. 73, no. 13, pp. 1781-1784, 1994. [\[Crossref\]](#)
16. J. Lu, G. Chen, D. Cheng, "A New Chaotic System and Beyond: the Generalized Lorenz-like System", *Int J Bifurcation Chaos*, vol. 14, no. 5, pp. 1507-1537, 2004. [\[Crossref\]](#)
17. V. Sundarapandian, I. Pehlivan, "Analysis, control, synchronization, and circuit design of a novel chaotic", *Mathematical and Computer Modelling*, vol. 55, pp. 1904-1915, 2012. [\[Crossref\]](#)
18. Q. Lai, A. Akgul, C. Li, G. Xu, Ü. Çavusoglu, "A New Chaotic System with Multiple Attractors", *Entropy*, vol. 2018, p. 15, 2017.
19. Y. B. Huang, S. H. Wang, Y. Wang, H. Li, "A New Four-Dimensional Chaotic System and Its Application in Speech Encryption", In *Information Communication Technologies Conference*, 2020. [\[Crossref\]](#)
20. C. Zhu, Y. Liu, Y. Guo, "Theoretic and Numerical Study of a New Chaotic System", *Intelligent Information Management*, vol. 2, pp. 104-109, 2010. [\[Crossref\]](#)
21. S. Vaidyanathan, A. Sambas, M. Mamat, W. Mada Sanjaya, "A new three-dimensional chaotic system with a hidden attractor, circuit design and application in wireless mobile robot", *Arch Control Sci*, vol. 27(LXIII), no. 4, pp. 551-554, 2017. [\[Crossref\]](#)
22. Q. Lai, P. D. K. Kuate, F. Liu, H. H. C. Lu, "An Extremely Simple Chaotic System with infinitely many coexisting attractors", *IEEE Transactions on Circuits and Systems II: Express Briefs*, vol. 67, no.6, pp. 1129-1133, 2019. [\[Crossref\]](#)
23. M. Sharafi, F. Fotouhi-Ghazvini, M. Shirali, M. Ghassemian, "A Low Power Cryptography Solution Based on Chaos Theory in Wireless Sensor Nodes", *IEEE Access*, vol. 7, pp. 8737-8753, 2019. [\[Crossref\]](#)
24. B. Triandi, E. Ekadiansyah, R. Puspasari, L. T. Iwan, F. Rahmad, "Improve Security Algorithm Cryptography Vigenere Cipher Using Chaos Functions", in *6th International Conference on Cyber and IT Service Management (CITSM)*, Parapat, Indonesia, 2018. [\[Crossref\]](#)

25. Y. Liu, Z. Jiang, X. Xu, F. Zhang, J. Xu, "Optical image encryption algorithm based on hyper-chaos and public-key cryptography", *Optics & Laser Technology*, vol. 127, no. 106171, 2020. [\[Crossref\]](#)
26. M. Lawnik, "Generalized logistic map and its application in chaos based cryptography," in *Journal of Physics: Conference Series*, Volume 936, 6th International Conference on Mathematical Modelling in Physical Sciences (IC-MSQUARE 2017), Pafos, Cyprus, 2017. [\[Crossref\]](#)
27. P. Antonik, M. Gulina, J. Pauwels, S. Massar, "Using a reservoir computer to learn chaotic attractors, with applications to chaos synchronization and cryptography", *Phys Rev*, vol. 98, no. 1, pp. 012215-012224, 2018. [\[Crossref\]](#)
28. R. Wang, P. Du, W. Zhong, H. Han, H. Sun, "Analyses and Encryption Implementation of a New Chaotic System", *Complexity*, vol. 2020, 2020. [\[Crossref\]](#)
29. M. Irfan, A. Asim, M. A. K, M. Ehatisham-ul-Haq, S. N. M, A. Saboor, A. Waqar, "Pseudorandom Number Generator (PRNG) Design Using Hyper-Chaotic Modified Robust Logistic Map(HC-MRLM)", *Electronics*, vol. 9, no. 104, 2020. [\[Crossref\]](#)
30. K. Demir, S. Ergün, "An Analysis of Deterministic Chaos as an Entropy", *Entropy*, vol. 20, no. 957, 2018. [\[Crossref\]](#)
31. K. Demir, S. Ergün, "Security analysis of a random number generator based on a chaotic hyperjerk system", *EPL*, vol. 129, 2020. [\[Crossref\]](#)
32. A. V. Tutueva, E. G. Nepomuceno, A. I. Karimov, V. S. Andreev, D. N. Butusov, "Adaptive chaotic maps and their application to pseudo-random", *Chaos, Solitons and Fractals*, vol. 133, no. 109615, 2020. [\[Crossref\]](#)
33. P. Ayubi, S. Setayeshi, A. M. Rahman, "Deterministic chaos game: A new fractal based pseudo-random", *J Information Security App*, vol. 52, no. 102472, 2020. [\[Crossref\]](#)
34. J. C. Sprott, W. J. Thio, "A Chaotic Circuit for Producing Gaussian", *Int J Bifurcation Chaos*, vol. 30, no. 8, 2020. [\[Crossref\]](#)
35. L. M. Pecora, T. L. Carroll, "Synchronization of chaotic systems", *Chaos: An Interdisciplinary Journal of Nonlinear Science*, vol. 25, no. 097611, 2015. [\[Crossref\]](#)
36. H. I. Deniz, Z. G. Cam Taskiran, H. Sedef, "Chaotic Lorenz Synchronization Circuit Design for Secure Communication," in 2018 6th International Conference on Control Engineering & Information Technology (CEIT), Istanbul, 2018. [\[Crossref\]](#)
37. K. M. Cuomo, A. V. Oppenheim, S. H. Strogatz, "Synchronization of Lorenz-based chaotic circuits with applications to communications", *IEEE Transactions on Circuits and Systems II: Analog and Digital Signal Processing*, vol. 40, no. 10, p. 626-633, 1993. [\[Crossref\]](#)
38. A. Sambas, W. S. Mada Sanjaya, M. Mamat and O. Tacha, "Design and numerical simulation of unidirectional chaotic synchronization and its application in secure communication system," *J Engineering Science and Technology Review*, vol. 6, no. 4, p. 66-73, 2013.
39. A. Rukhin, J. Soto, J. Nechvatal, M. Smid, E. Barker, "A statistical test suite for random and pseudorandom number generators for cryptographic applications", *Tech Rep, Booz-Allen and Hamilton Inc Mclean Va*, 2001. [\[Crossref\]](#)
40. A. N. Pisarchik, U. Feudel, "Control of multistability", *Physics Reports*, vol. 540, no. 4, pp. 167-218, 2014. [\[Crossref\]](#)
41. R. C. Hilborn, Amanda, L. Cross, *Chaos and Nonlinear Dynamics: An Introduction for Scientists and Engineers*, New York: Oxford University Press, 2004.
42. A. Wolf, J. B. Swift, H. L. Swinney, J. A. Vastano, "Determining Lyapunov exponents from a time series", *Physica*, vol. 16, no. D, pp. 285-317, 1985. [\[Crossref\]](#)
43. A. Bedri Özer, E. Akın, "Tools for Detecting Chaos", *Sakarya Üniversitesi Fen Bilimleri Enstitüsü Dergisi*, vol. 9, no. 1, pp. 60-66, 2005.
44. Analog Devices, AD633 Low Cost Analog Multiplier, rev. K. 2015.
45. Analog Devices, AD844 60 MHz 2000 V/us Monolithic Op Amp, rev. F. 2009.
46. E. Tlelo-Cuautle, J. D. Díaz-Muñoz, A. M. González-Zapata, R. Li, W. D. León-Salas, F. V. Fernández, O. Guillén-Fernández, I. Cruz-Vega, "Chaotic image encryption using hopfield and hindmarsh-rose neurons implemented on FPGA", *Sensors*, vol. 20, no. 5, pp. 1326, 2020. [\[Crossref\]](#)
47. R. Trejo-Guerra, E. Tlelo-Cuautle, J. M. Jimenez-Fuentes, C. Sánchez-López, J. M. Muñoz-Pacheco, G. Espinosa-Flores-Verdad, J. M. Rocha-Perez, "Integrated circuit generating 3-and 5-scroll attractors", *Communications in Nonlinear Science and Numerical Simulation*, vol. 17, no.11, pp. 4328-4335, 2012. [\[Crossref\]](#)
48. R. Trejo-Guerra, E. Tlelo-Cuautle, C. Cruz-Hernández, C. Sanchez-Lopez, "Chaotic communication system using Chua's oscillators realized with CCLII+ s", *Int J Bifurcation Chaos*, vol. 19, no.12, pp. 4217-4226, 2009. [\[Crossref\]](#)
49. B. Muthuswamy, "Implementing memristor based chaotic circuits", *Int J Bifurcation Chaos*, vol. 20, no. 05, pp. 1335-1350, 2010. [\[Crossref\]](#)





Abdullah Noor, received his B.Sc. degree in Electronics Engineering from International Islamic University Islamabad, Pakistan in 2019. He is currently pursuing Masters in Electronics and Communication Engineering at Yıldız Technical University Istanbul, Turkey. His research interests include artificial intelligence, neural networks, and chaotic circuits and its applications.



Zehra Gülru Çam Taşkıran, received her B.Sc. and M.Sc. degrees in Electronics Engineering from Istanbul Technical University, Istanbul, Turkey in 2011 and 2013, respectively. She received her PhD degree in Electronics and Communications Engineering from Yıldız Technical University, Istanbul, Turkey, in 2018. Between 2013 and 2018, she was a research assistant and since September, 2018, she is an assistant professor in the Department of Electronics and Communications Engineering at Yıldız Technical University, Istanbul, Turkey. Dr. Cam Taskiran's current research interests are in the areas of circuit theory, nonlinear circuits, memristive circuits, and chaotic circuits.